Neuropsychopharmacology www.nature.com/npp

ARTICLE

Network-based functional connectivity predicts response to exposure therapy in unmedicated adults with obsessive–compulsive disorder

Tracey C. Shi[1,2], David Pagliaccio[1], Marilyn Cyr[1], H. Blair Simpson[1,2] and Rachel Marsh[1,2]

Obsessive–compulsive disorder (OCD) is associated with alterations in cortico-striato-thalamo-cortical brain networks, but some resting-state functional magnetic resonance imaging studies report more diffuse alterations in brain connectivity. Few studies have assessed functional connectivity within or between networks across the whole brain in unmedicated OCD patients or how patterns of connectivity predict response to exposure and ritual prevention (EX/RP) therapy, a first-line treatment for OCD. Herein, multiband resting-state functional MRI scans were collected from unmedicated, adult patients with OCD ($n = 41$) and healthy participants ($n = 36$); OCD patients were then offered twice weekly EX/RP (17 sessions). A whole-brain-network-based statistic approach was used to identify group differences in resting-state connectivity. We detected altered pre-treatment functional connectivity between task-positive regions in the temporal gyri (middle and superior) and regions of the cingulo-opercular and default networks in individuals with OCD. Signal extraction was performed using a reconstruction independent components analysis and isolated two independent subcomponents (IC1 and IC2) within this altered connectivity. In the OCD group, linear mixed-effects models tested whether IC1 or IC2 values predicted the slope of change in Yale–Brown Obsessive–Compulsive Scale (Y-BOCS) scores across EX/RP treatment. Lower (more different from controls) IC2 score significantly predicted greater symptom reduction with EX/RP (Bonferroni-corrected $p = 0.002$). Collectively, these findings suggest that an altered balance between task-positive and task-negative regions centered around temporal gyri may contribute to difficulty controlling intrusive thoughts or urges to perform ritualistic behaviors.

Neuropsychopharmacology (2021) 46:1035–1044; https://doi.org/10.1038/s41386-020-00929-9

INTRODUCTION

Obsessions and compulsions are the hallmarks of obsessive–compulsive disorder (OCD) and are thought to result from disruption of cortico-striato-thalamo-cortical (CSTC) feedback loops, specifically involving the anterior cingulate cortex, orbito-frontal cortex, and other frontoparietal regions [1–7]. The CSTC model has been investigated using resting-state functional magnetic resonance imaging (rsfMRI), which delineates brain connection-level or network-level functioning independent from a specific task. Most rsfMRI studies of OCD have focused on a priori subcortical (striatal) seed regions of interest (ROIs) and report alterations in frontal-subcortical connectivity in adults with OCD, consistent with the CSTC model [8–11]. These studies, however, differ in their specific findings (i.e., increased versus decreased connectivity in OCD) and many included medicated participants. Few studies have assessed functional connectivity within or between networks across the whole brain in unmedicated adults with OCD or examined how patterns of connectivity predict response to exposure and ritual prevention therapy (EX/RP), a first-line treatment for OCD.

Neuroimaging studies have begun examining disruptions extending beyond traditional CSTC loops in OCD [12–16]. Whole-brain studies of rsfMRI connectivity across large-scale intrinsic brain networks in unmedicated OCD participants have revealed broader alterations across task-positive and task-negative networks [17, 18]. "Task-positive" networks, including the fronto-parietal (FPN), cingulo-opercular (CO), and ventral attention (VAN) networks, are typically engaged during goal-directed tasks requiring cognitive control and attention [19–21]. Of these task-positive networks, the CO functions to arbitrate how attention is divided among tasks and is alternatively referred to as a "salience" network [22]. The default-mode network (DMN) is a "task-negative" network, typically engaged during rest, self-referential processes, and mind wandering [23–29]. Findings from rsfMRI studies using seeds in or analyses restricted to the DMN, FPN, and salience/CO also suggest abnormal connectivity in OCD within and among these networks [30, 31]. Notably, previous whole-brain studies of adults [17] and children [18] reported decreased connectivity between and within these networks in OCD, while studies that focused exclusively on these networks [30, 31] reported increased connectivity across them. Also notable is that these prior studies included small samples ranging from 17 [17] to 35 [30] participants with OCD. Such findings suggest that OCD pathology may involve an impaired functional balance among

[1]Department of Psychiatry, New York State Psychiatric Institute, 1051 Riverside Drive, Unit 74, New York, NY 10032, USA and [2]Department of Psychiatry, Columbia University Irving Medical Center, 1051 Riverside Drive, Unit 74, New York, NY 10032, USA
Correspondence: Tracey C. Shi (ts2928@cumc.columbia.edu)
These authors contributed equally: H. Blair Simpson, Rachel Marsh

Received: 12 August 2020 Revised: 30 October 2020 Accepted: 20 November 2020
Published online: 14 January 2021

task-positive and task-negative networks. For example, pediatric OCD findings from our lab [18] and meta-analytic findings from adults [6] suggest that the "triple network" model of psychopathology might apply to OCD, wherein the salience/CO might inappropriately "switch" or modulate between task-positive networks and the task-negative DMN [6, 18].

Probing whole-brain rsfMRI connectivity in adults may thus expand our understanding of the neurobiology of OCD beyond the CSTC model. However, the different methods used across previous studies complicate drawing conclusions about functional abnormalities in OCD, in part because findings from studies that analyze different brain regions are difficult to reconcile. For example, a study that does not include a particular ROI in analyses cannot be compared to studies with findings in that ROI. While a priori ROI selection can provide evidence for specific hypotheses such as the CSTC model, whole-brain approaches with good statistical power are necessary to search for more broad neural dysfunction across the brain.

RsfMRI studies have also begun to examine neural predictors of OCD treatment response. Cognitive-behavioral therapy (CBT) consisting of EX/RP is an evidence-based treatment for OCD. Although EX/RP has proven highly effective in randomized controlled trials, individual patients range in the degree of their response [32, 33]. Given the substantial investment of time and cost associated with EX/RP, the ability to predict which patients are likely to respond best could substantially improve clinical efficiency [34]. Prior rsfMRI findings suggest that EX/RP response can be predicted by changes in multiple brain areas, including the ventromedial prefrontal cortex [35] and DMN regions [36]. However, these studies included medicated patients despite data indicating that medication may affect neural activity in OCD [37]. Moreover, both studies focused on specific brain regions or networks defined a priori based on their established association with OCD, thereby precluding detection of abnormalities that do not overlap with regions identified in previous work. Two additional studies used whole-brain graph theoretical approaches to address the latter problem, but both used relatively small sample sizes [38, 39] (both $n = 17$) and the former also included medicated patients. As with the rsfMRI literature regarding neural changes in OCD, the heterogeneity in methods employed and in the OCD samples studied limits the ability to draw conclusions across studies about EX/RP response prediction.

To address this gap in the literature, we used a whole-brain approach in a larger sample of unmedicated patients to investigate patterns of functional connectivity that differ between adults with OCD and healthy controls (HC) and also predict EX/RP response in OCD patients. We used state-of-the-art multiband MRI acquisition sequences, taking advantage of recent advances in spatial and temporal resolution, and a whole-brain network-based statistic (NBS) technique to identify abnormalities in resting-state functional connectivity (rs-FC) in unmedicated adults with OCD. We then used these group differences to predict response to EX/RP in the OCD group. Based on previous findings from unmedicated participants with OCD, we hypothesized that the functional balance across task-positive and task-negative regions would be altered in OCD, and that such alterations would predict EX/RP response.

METHODS AND MATERIALS

Participants

Details of participant recruitment and data collection are published elsewhere [40]. Briefly, unmedicated adults with OCD and age-, sex-, and race/ethnicity-matched HC were recruited from the New York City area. All patients met Diagnostic and Statistical Manual of Mental Disorders, Fifth Edition [41] criteria for OCD as confirmed by trained raters using the Structured Clinical Interview for Diagnostic and Statistical Manual-IV-TR Axis I Disorders [42]. Healthy participants had no lifetime psychiatric disorders. Participants were excluded for MRI contraindications, history of neurological illness or seizures, head trauma with loss of consciousness, pervasive developmental disorder, any current psychiatric diagnosis (other than OCD or phobias [if secondary] for the OCD group), or an estimated IQ < 80. The study was approved by the Institutional Review Board of the New York State Psychiatric Institute (NYSPI). All participants provided written informed consent.

Treatment

Patients received a standardized protocol of EX/RP [43] that included 17 sessions (2 introductory and 15 exposure sessions, each 90-min long) delivered twice weekly by a clinical psychologist. Exposure sessions consisted of therapist-aided exposures, ritual prevention, and education about relapse prevention.

Clinical measures

Severity of OCD symptoms was assessed pre-, mid-, and post-treatment by a trained rater (independent from the treating clinician) using the Yale–Brown Obsessive Compulsive Scale (Y-BOCS) [44].

MRI acquisition

High-resolution MRI scans were conducted at NYSPI using sequences adapted from the Human Connectome Project (HCP) [45] for a GE Signa 3T MR750 scanner (details in Supplement). Briefly, each participant completed T1- and T2-weighted structural images and 2 runs of multiband resting-state functional MRI (repetition time = 850 ms, multiband factor = 6, 2 mm isotropic voxels = 7 min and 32 s per run). For the resting-state scans, participants were instructed to relax with their eyes open and remain awake.

MRI pre- and post-processing

Functional data were preprocessed using the HCP pipelines v3.4 [46] (details in Supplement and Fig. S1). First-level analyses were performed in "grayordinate" space ("91k" CIFTI format), which combines cortical surface and subcortical volume representations. Post-processing was performed in Matlab R2019a (Mathworks, 2019). Nuisance regression was performed with 24 motion parameters (bandpass filtered [47]) and four average global grayordinate signal parameters, including squared terms, temporal derivatives, and squared temporal derivatives for all motion and global mean regressors [48]. Motion censoring [49, 50] based on framewise displacement (FD; >0.25 mm) and DVARS (*z*-score > 3) was also performed. All participants had at least 495 frames (7 min) of data remaining after censoring.

The brain was divided into 352 cortical and subcortical regions using a publicly available CIFTI-space segmentation (https://balsa.wustl.edu/file/show/JX5V) using HCP Connectome Workbench [51]. This segmentation included 333 cortical parcels from the Cortical Area Parcellation atlas defined by homogeneity of rs-FC [52] and 19 anatomically defined subcortical ROIs from the Freesurfer Subcortical Atlas: left and right amygdala, hippocampus, accumbens, caudate, pallidum, putamen, thalamus, ventral diencephalon, cerebellum, and brain stem. Next, the BOLD timeseries from each of the 352 regions/parcels ("nodes") was extracted and correlated with all other nodes. These correlations ("edges") were Fisher r-to-z transformed, resulting in a 352×352 connectivity matrix for each participant.

A growing consensus suggests that whole-brain analyses are sensitive to how the brain is parcellated and the granularity of these parcels [53, 54]. To test robustness of our NBS analyses (described below), we conducted a sensitivity analysis aimed to replicate findings using a coarser 100-parcel segmentation [55] (Supplement). In addition to having a substantially different number and granularity of ROIs, this parcellation was created

using a different reference dataset, modeled using an algorithm accounting for both homogeneity and local gradient changes, and trained on both task and resting-state fMRI data.

Statistical analysis

Participant characteristics. Group differences in participant characteristics were tested using *t*-tests for continuous variables and χ^2 tests for categorical variables in Matlab.

Group differences in functional connectivity. Whole-brain correlation matrices were examined for group differences between OCD patients and controls using the Network Based Statistic (NBS Connectome v1.2 [56]). NBS uses permutation testing to identify significant components or "clusters" of contiguous region-to-region connections and to correct for multiple comparisons (10,000 permutations), which can control the family-wise error rate with more power than mass univariate testing in cases where the brain connectivity features of interest are interconnected [56] (see Supplement).

Group differences were tested using an F-test to examine both OCD > HC and OCD < HC differences parsimoniously in one test (rather than two unidirectional t-tests), controlling for age, sex, and mean FD to control for residual effects of head motion during the MRI scan. Extent thresholding and an f-statistic threshold of 14 ($p = 0.0004$) were used for primary analyses. Findings from NBS with extent and intensity thresholding across a range of f-statistic thresholds are reported in the supplement. Significant components were visualized using the BrainNet Viewer [57].

As NBS defines components based on their interconnectedness and we examined an F-test (rather than directional *t*-tests), a given component identified in our analysis may include functionally distinct subcomponents that may even show different direction of effects. Therefore, we used reconstruction independent components analysis (RICA) [58] to isolate distinct independent (sub) components (IC) within the NBS results (details in Supplement). For each participant, a value for each IC was calculated as a weighted average across all edges, weighted by their RICA loadings. Two-sample t-tests were used to test the significance of group differences in resultant ICs. Critically, this allowed for more parsimonious follow-up testing rather than running analyses for each identified edge.

NBS is designed to identify components that are significant in the aggregate, but the individual edges cannot be interpreted in isolation from the component [56]. Following our prior work with youth with OCD [18], we performed a supplemental group analysis using an FDR-corrected mass univariate approach. This approach has less power (than NBS) to detect interconnected significant edges but permits the investigation of individual edges (detailed in Supplement).

Response to treatment. Analyses examined associations between the functional connectivity that was identified as different across groups (ICs, described above) and response to treatment in patients with OCD. For each IC, a linear mixed-effect (LME) model ("lme4" package [59]) was conducted in R v3.6.1 (R Core Team, 2019) with Y-BOCS scores as a repeated-measure dependent variable; a random effect for participant; and fixed effects for age, sex, mean head motion (FD), time of assessment (week 0, 4, or 8), component score for the IC, and the interaction between time and IC score. The main effect of time indicated the slope of Y-BOCS change across pre-, mid-, and post-treatment. A main effect of IC score would indicate an association with pre-treatment (week 0) Y-BOCS scores. The IC × time interaction was the predictor of interest, indicating that the slope of change in Y-BOCS scores over treatment differed as a function of baseline rs-FC. This interaction effect was Bonferroni-corrected for multiple comparisons across ICs.

RESULTS

Participant characteristics

Eighty-eight adult participants (47 with OCD and 41 HCs) provided consent for and were enrolled in the study. Six participants ($n = 3$ OCD; $n = 3$ HC) did not complete the MRI scan and five ($n = 3$ OCD; $n = 2$ HC) were excluded from analysis due to incidental anatomical findings, excessive head motion during the structural scan, or technical issue with the scanner. Two HC participants had only one run of resting-state data; the remaining participants completed two runs.

Demographic and clinical characteristics of the 77 participants ($n = 41$ OCD; $n = 36$ HC) included in the final analyses are shown in Table 1. All patients were either psychotropic medication naïve (34 out of 41 patients) or free from psychotropic medication for an average of 126 weeks (range 9–676 weeks) prior to the MRI scan.

Treatment outcomes

The majority of patients (76%) completed at least 14 sessions of EX/RP, with 25 out of 41 patients (61%) completing all 17 (median = 17 sessions, mean = 14.1, SD = 5.1, range = 1–17). Of the 41 patients included in analyses, 1 did not complete the mid-treatment evaluation (week 4), 2 did not complete the post-treatment evaluation (week 8), and 3 did not complete either the mid-treatment or post-treatment evaluations (all female). The number of EX/RP sessions completed was not associated with age, baseline Y-BOCS severity, or head motion, though males tended to complete more treatment sessions. Y-BOCS scores declined substantially over the course of treatment (mean decrease = 11.5 points, SD = 8.0).

Resting-state functional connectivity (rs-FC)

Group differences. NBS revealed one component with significantly altered connectivity in patients relative to controls ($p = 0.027$). This component consisted of 23 edges, primarily between parcels in the right VAN, the salience/CO and the DMN (Table 2 and Fig. 1). Specifically, the right middle and superior temporal gyri formed a hub in this component, with three nodes in these gyri (all mapped to the VAN) that collectively appeared in 21 of the 23 edges. These edges primarily showed reduced connectivity

Table 1. Demographic and clinical characteristics.

	Healthy ($n = 36$)	OCD ($n = 41$)	Group difference test statistic
Age	29.7 (7.5)	29.1 (7.3)	$t = -0.37$
Sex, male	18 (50%)	21 (51%)	$\chi^2 = 0.01$
Race, white	26 (72%)	30 (73%)	$\chi^2 = 0.01$
Handedness, right	32 (89%)	33 (80%)	$\chi^2 = 1.30$
Education, years	16.6 (1.7)	16.1 (2.0)	$t = -1.03$
IQ	111.7 (12.0)	106.0 (13.1)	$t = -1.96$
Y-BOCS score pretreatment	–	24.8 (3.5)	–
Y-BOCS score posttreatment[a]	–	12.9 (7.9)	–
Resting-state fMRI			
Frames cut, %	4.9% (1.2%)	4.9% (1.3%)	$t = 0.06$
Mean FD	0.03 (0.02)	0.03 (0.02)	$t = 0.31$

There were no significant group differences in demographic characteristics or head motion during resting-state acquisition. Parentheses after numbers contain standard deviation for continuous variables or percentage of total for discrete variables. Percentage of frames cut indicates the average percentage of frames regressed as motion or timeseries outliers, and mean framewise displacement (FD) indicates average head motion only among runs included in analyses.

[a]Values for $n = 36$ patients who completed post-treatment follow-up session.

Table 2. Resting-state functional connectivity group differences.

Parcel 1[a]			Parcel 2[a]			Mean edge values	
Parcel name	Description	Center (MNI)	Parcel name	Description	Center (MNI)	OCD	Controls
L_CinguloOperc_10	Insula	−38.0 6.3 10.1	L_None_18	Temporal lobe, sub-gyral	−40.5 −14.1 −26.9	−0.18	0.05
L_DorsalAttn_17	Middle frontal gyrus	−36.8 43.1 15.4	L_CinguloOperc_2	Cingulate gyrus	−8.4 −5.0 44.2	0.07	0.25
R_VentralAttn_12	Middle temporal gyrus	59.8 −40.0 4.2	L_CinguloOperc_10	Insula	−38.0 6.3 10.1	−0.03	0.20
R_VentralAttn_12	Middle temporal gyrus	59.8 −40.0 4.2	R_CinguloOperc_33	Insula	37.4 4.7 13.0	−0.06	0.20
R_VentralAttn_12	Middle temporal gyrus	59.8 −40.0 4.2	L_Auditory_10	Postcentral gyrus	−50.2 −16.4 16.1	−0.04	0.15
R_VentralAttn_12	Middle temporal gyrus	59.8 −40.0 4.2	R_Auditory_22	Postcentral gyrus	54.5 −14.1 17.4	−0.06	0.13
R_VentralAttn_13	Middle temporal gyrus	57.2 −34.2 −2.4	L_Default_7	Superior occipital gyrus	−41.0 −76.0 33.7	0.19	−0.06
R_VentralAttn_13	Middle temporal gyrus	57.2 −34.2 −2.4	R_Default_27	Middle temporal gyrus	60.9 −25.7 −7.8	0.79	0.54
R_VentralAttn_13	Middle temporal gyrus	57.2 −34.2 −2.4	L_CinguloOperc_2	Cingulate gyrus	−8.4 −5.0 44.2	−0.28	−0.06
R_VentralAttn_13	**Middle temporal gyrus**	**57.2 −34.2 −2.4**	**L_CinguloOperc_10**	**Insula**	**−38.0 6.3 10.1**	**−0.28**	**0.00**
R_VentralAttn_13	Middle temporal gyrus	57.2 −34.2 −2.4	L_CinguloOperc_13	Insula	−31.0 23.0 6.1	−0.24	0.00
R_VentralAttn_13	Middle temporal gyrus	57.2 −34.2 −2.4	R_CinguloOperc_27	Medial frontal gyrus	8.2 −1.5 63.0	−0.21	0.01
R_VentralAttn_13	Middle temporal gyrus	57.2 −34.2 −2.4	R_CinguloOperc_30	Inferior parietal lobule	55.3 −27.8 29.5	−0.25	0.01
R_VentralAttn_13	**Middle temporal gyrus**	**57.2 −34.2 −2.4**	**R_CinguloOperc_33**	**Insula**	**37.4 4.7 13.0**	**−0.26**	**−0.01**
R_VentralAttn_13	Middle temporal gyrus	57.2 −34.2 −2.4	R_CinguloOperc_37	Insula	35.7 24.0 7.3	−0.18	0.07
R_VentralAttn_13	Middle temporal gyrus	57.2 −34.2 −2.4	R_CinguloOperc_38	Insula	48.2 2.2 6.4	−0.21	0.05
R_VentralAttn_13	Middle temporal gyrus	57.2 −34.2 −2.4	L_MedialParietal_3	Precuneus	−12.0 −70.0 44.8	−0.20	0.01
R_VentralAttn_13	**Middle temporal gyrus**	**57.2 −34.2 −2.4**	**R_Visual_38**	**Cuneus**	**6.5 −77.8 28.4**	**−0.26**	**−0.03**
R_VentralAttn_13	Middle temporal gyrus	57.2 −34.2 −2.4	L_SMmouth_2	Precentral gyrus	−40.6 −11.6 48.2	−0.20	−0.01
R_VentralAttn_13	Middle temporal gyrus	57.2 −34.2 −2.4	R_SMmouth_6	Precentral gyrus	43.5 −11.1 45.2	−0.22	0.00
R_VentralAttn_16	Superior temporal gyrus	47.3 −34.7 2.3	L_CinguloOperc_16	Inferior parietal lobule	−59.0 −23.4 33.5	−0.18	0.02
R_VentralAttn_16	Superior temporal gyrus	47.3 −34.7 2.3	R_CinguloOperc_30	Inferior parietal lobule	55.3 −27.8 29.5	−0.02	0.20
R_VentralAttn_16	Superior temporal gyrus	47.3 −34.7 2.3	R_CinguloOperc_34	Claustrum	38.5 9.9 −0.6	−0.02	0.18

This table details the 23 edges that comprised the NBS component with a significant group difference between patients with OCD and healthy controls (also shown in Fig. 1). Edges are identified by the nodes (parcels) they connect. Parcel names are those used by the BALSA database (https://balsa.wustl.edu/file/show/JX5V). Center (MNI) values are the coordinates of the center of mass for each parcel. Parcel descriptions are assigned using the Talairach Daemon (http://talairach.org/daemon.html) [85, 86]. Bold indicates edges that were also significant using the FDR-corrected mass univariate approach (Table S3).
[a]All edges are undirected. Parcels are numbered as 1 and 2 simply for reference; this does not indicate directionality of the connection.

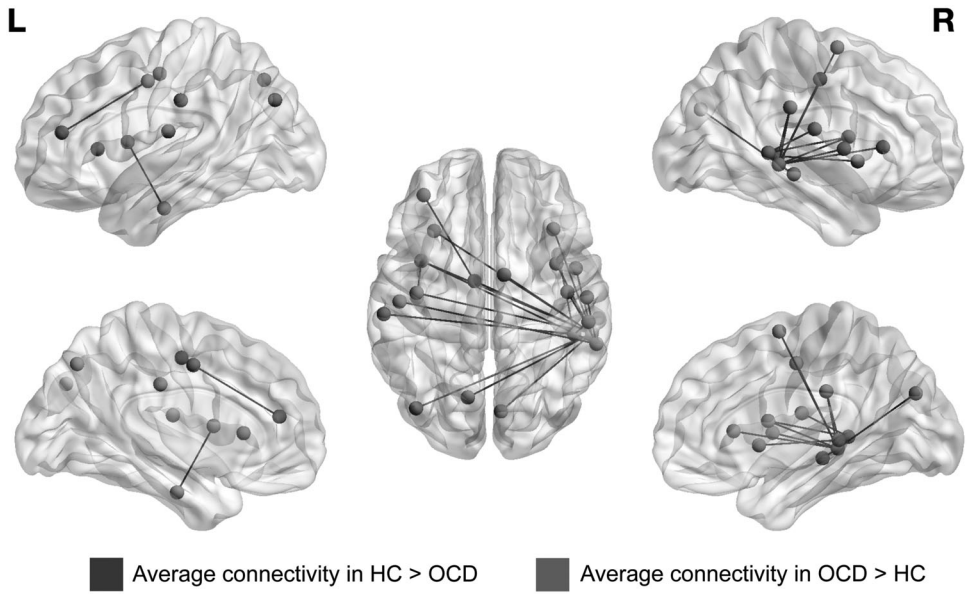

Fig. 1 Resting-state functional connectivity group differences. Visualization of the 23 edges comprising the NBS component that differed significantly across patients with OCD and healthy controls (details in Table 2). Nodes (endpoints of edges) are plotted by center of mass. Edges (21) with greater average connectivity in healthy controls (HC) compared to the OCD group are represented in blue. Edges (2) with greater average connectivity in the OCD group are represented in red.

in OCD relative to HC participants with negative connectivity in OCD and near zero connectivity in HC. The remaining two edges connecting the middle temporal gyrus (MTG, mapped to VAN) to DMN nodes showed greater connectivity in the OCD group (Table 2). NBS with the contrasting Schaefer parcellation similarly revealed one significant component with a hub in the right temporal lobe ($p = 0.017$, Supplement). The mass univariate analysis revealed seven edges that differed significantly across groups after FDR-correction (see Supplemental text and Table S3); three of these edges overlapped with the significant NBS component (bolded in Table 2).

To address heterogeneity in the identified NBS component, characterize these group differences parsimoniously, and avoid conducting 23 separate post hoc analyses, we used a standard signal extraction method (RICA, see "Methods and materials") to reduce the 23 edges into two independent subcomponents (Table 3 and Fig. 2). Both independent subcomponent 1 (IC1) and independent subcomponent 2 (IC2) were significantly lower in the OCD relative to HC group (IC1: $t = -6.9$, $p < 10^{-8}$; IC2: $t = -5.8$, $p < 10^{-6}$).

Predicting treatment response. Among participants with OCD, LME analyses revealed that only IC2 significantly predicted Y-BOCS trajectory over the course of EX/RP. Specifically, a model predicting Y-BOCS as a repeated-measure dependent variable revealed a significant IC × time interaction for IC2 ($p = 0.002$ after Bonferroni correction; Table 4), but not IC1 (corrected $p = 0.84$), such that participants with lower (more different from HC) IC2 showed greater improvement in symptoms. None of the three edges that were identified by both NBS and the mass univariate analysis predicted treatment response individually (see Supplement). In the subsets of subjects who completed at least 14 or all 17 of the EX/RP treatment sessions, LME analyses replicated the full sample results that IC2 ($p = 0.001$ after Bonferroni correction for 14-session subset; $p = 0.002$ for 17-session subset), but not IC1 (corrected $p = 0.54$ for 14 sessions; $p = 0.10$ for 17 sessions), significantly predicted Y-BOCS trajectory over the course of EX/RP. These results were similar with and without inclusion of the number of CBT sessions as a covariate.

Sensitivity analyses using Schaefer parcellation. NBS with the contrasting Schaefer parcellation revealed one significant component with a hub in the right temporal lobe ($p = 0.017$, Supplement). Since all of these edges had decreased rs-FC on average in OCD relative to HC, we performed RICA with 1 subcomponent. This subcomponent did not significantly predict Y-BOCS change over treatment. Finally, the mass univariate analysis (FDR-corrected F tests) using the Schaefer parcellation revealed two edges that significantly differed across groups, neither of which overlapped with the significant NBS component (Supplement).

DISCUSSION

Using a data-driven, whole-brain approach, we detected altered functional connections between middle and superior temporal gyri nodes within the VAN and regions within the salience/CO and DMN in unmedicated patients with OCD. Moreover, these alterations positively predicted response to EX/RP. These data suggest that in unmedicated individuals with OCD, altered communication between task-positive and task-negative regions may contribute to the impaired control over intrusive thoughts and urges to perform rituals instead of more adaptive goal-directed behaviors.

Group differences between OCD and HC

Our findings of altered connectivity between nodes in task-positive (i.e., VAN and salience/CO) and task-negative (i.e., DMN) networks in OCD seem to conform with findings from previous resting-state studies of unmedicated adults [17, 30, 31] and youth [18] with OCD reporting aberrant connectivity between task-positive and task-negative regions. Of note, only two of the edges in our significant NBS component involved the DMN, and other edges varied in the patterns of connectivity (i.e., negative or positive across groups; greater or reduced in OCD). Thus, future research with larger samples is required to confirm any network-based interpretation of altered functional connectivity in OCD. Prior findings suggest both increased [60, 61] and decreased [17, 18, 62] connectivity across task-positive and -negative networks in OCD, possibly due to the use of different analysis

Table 3. Edge weights for each independent subcomponent.

Parcel 1[a] name	Parcel 2[a] name	Weight in independent component 1	Weight in independent component 2
L_CinguloOperc_10	L_None_18	0.14	0.12
L_DorsalAttn_17	L_CinguloOperc_2	−0.06	0.16
R_VentralAttn_12	L_CinguloOperc_10	0.08	0.32
R_VentralAttn_12	R_CinguloOperc_33	0.10	0.30
R_VentralAttn_12	L_Auditory_10	0.05	0.20
R_VentralAttn_12	R_Auditory_22	0.08	0.16
R_VentralAttn_13	L_Default_7	−0.19	−0.16
R_VentralAttn_13	R_Default_27	−0.53	0.57
R_VentralAttn_13	L_CinguloOperc_2	0.26	−0.04
R_VentralAttn_13	L_CinguloOperc_10	0.28	0.09
R_VentralAttn_13	L_CinguloOperc_13	0.25	0.12
R_VentralAttn_13	R_CinguloOperc_27	0.22	0.06
R_VentralAttn_13	R_CinguloOperc_30	0.25	0.10
R_VentralAttn_13	R_CinguloOperc_33	0.26	0.10
R_VentralAttn_13	R_CinguloOperc_37	0.22	0.26
R_VentralAttn_13	R_CinguloOperc_38	0.25	0.18
R_VentralAttn_13	L_MedialParietal_3	0.10	−0.02
R_VentralAttn_13	R_Visual_38	0.20	−0.05
R_VentralAttn_13	L_SMmouth_2	0.16	−0.08
R_VentralAttn_13	R_SMmouth_6	0.20	−0.04
R_VentralAttn_16	L_CinguloOperc_16	0.14	0.11
R_VentralAttn_16	R_CinguloOperc_30	0.08	0.32
R_VentralAttn_16	R_CinguloOperc_34	0.05	0.27

Weights (loadings) calculated by reconstruction independent components analysis (also shown in Fig. 2).
[a]All edges are undirected. Parcels are numbered as 1 and 2 simply for reference; this does not indicate directionality of the connection.

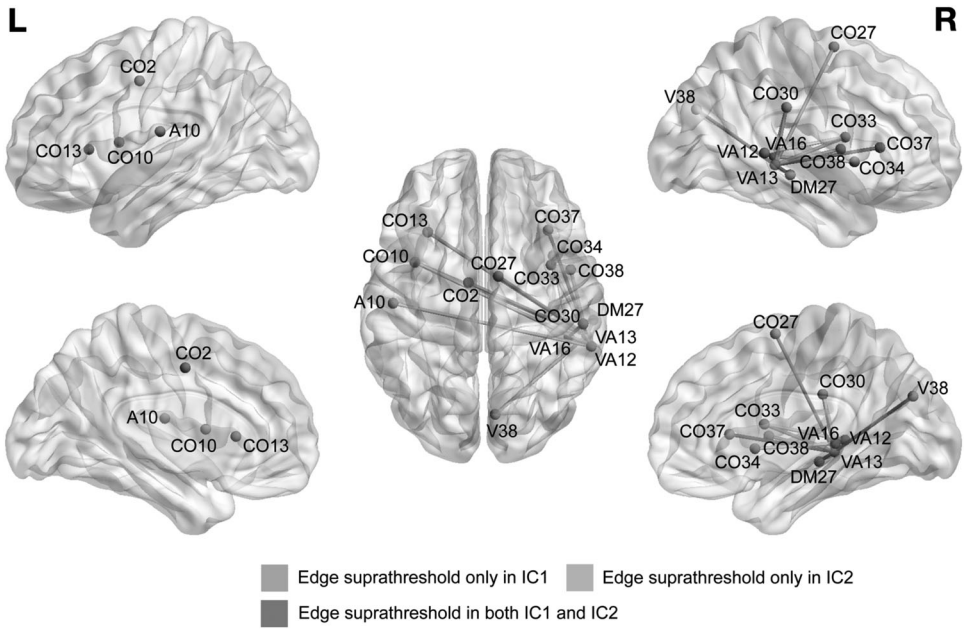

Fig. 2 Visualization of the largest weights (loadings) generated by reconstruction independent components analysis (RICA) for independent subcomponents 1 and 2 (see also Table 3). Nodes (endpoints of edges) are plotted by center of mass. Edges are color-coded according to the subcomponent(s) for which they have a suprathreshold RICA weighting. An edge is defined as "suprathreshold" for a subcomponent(s) if the absolute value of its RICA weight in the subcomponent is >0.2. A auditory, CO cingulo-opercular, DM default mode, V visual, VA ventral attention.

Table 4. Fitted coefficients for LME model predicting Y-BOCS as a repeated dependent measure.

Fixed effects	Coefficient	*T* value	*P* value (uncorrected)
(Intercept)	23.1	6.6	$<10^{-7}$
Timepoint	−1.7	−11.9	$<10^{-15*}$
IC2 strength	0.5	0.19	0.85
Timepoint × IC2 strength interaction	1.2	3.4	0.0011*
Age	0.04	0.38	0.71
Male	−2.4	−1.5	0.15
Mean FD	48.6	0.97	0.34

Mean framewise displacement (FD) is used to control for residual head motion in the scanner. *P* values are displayed uncorrected for multiple comparisons.
*Significant at $p = 0.05$ threshold after Bonferroni correction for two comparisons (0.05/2 = 0.025).

methods across studies. Our data-driven results are consistent with prior whole-brain analyses that revealed primarily decreased connectivity in OCD [17, 18, 62]. Importantly, naming conventions for and divisions between task-positive networks are inconsistent across studies: different parcellation schemes combine these networks (e.g., as a single FPN, usually in older literature [63]) or label the same regions as part of the ventral attention [64], CO [22], or salience [65] networks. Such differences in nomenclature complicate comparison of findings across this literature. For example, the "FPN" referenced by one particular study may be the "CO" of another study, distinguishable only by the specific ROIs being studied rather than the network label. For this reason, we discuss and interpret our findings from anatomical ROIs rather than relying solely on network labeling.

Our significant NBS component included nodes in the insula, inferior parietal lobule (IPL), and cingulate, labeled as part of the CO network in the parcellation scheme used herein [52] but sometimes included more broadly in an overall FPN [63, 66] or referred to as the salience network [67]. Previous findings suggest altered insula [6, 17, 66, 68, 69], IPL [66], and cingulate [6, 60, 68–70] connectivity in OCD patients. For example, a meta-analysis of seed-based rsfMRI studies revealed reduced connectivity in OCD compared to control participants from insular seeds and general dysconnectivity from the DMN to anterior cingulate cortex [6]. Differences in the particular connections identified across the previous studies and ours are likely due to methodological differences. For example, all previous rs-FC studies of adult OCD except for one [71] used singleband acquisition sequences and processed images in volume space, whereas we used multiband acquisition and processed in CIFTI format to represent cortical regions as a surface. Studies also differ in the size and shape of ROIs (e.g., the 160-ROI Dosenbach atlas [12, 72] or ROIs derived from prior rsfMRI or task-based fMRI studies [66, 68]) and in whether resting-state data were acquired with participants' eyes open [17, 66] or closed [8, 12, 60, 68–70]. Despite these methodological variations, the high degree of convergence between our whole-brain results and earlier seed-based findings indeed suggests diffuse alterations in connectivity across the insula, IPL, and cingulate in OCD. Such dysconnectivity could contribute to the cognitive control deficits observed in OCD patients [73, 74] and their difficulty controlling or attending away from intrusive thoughts.

Our NBS analysis revealed reduced rs-FC in the OCD group particularly from right MTG to left cingulate, bilateral insula, IPL, and precentral gyrus. This functional connection is consistent with human anatomical connections (i.e., white matter tracts identified through diffusion-weighted imaging) between the MTG and IPL, lateral frontal areas, and other MTG subregions [75]. Previous functional findings including medicated and unmedicated patients suggest abnormal spontaneous resting-state activity (amplitude of low-frequency fluctuations) in the MTG in OCD [76]. Other seed-based analyses from unmedicated patients point to increased rs-FC between the MTG and raphe nucleus that associated with baseline symptoms and predicted poorer response to SSRIs [77]. We did not examine the raphe nucleus specifically since the subcortical parcellation used herein included one region for the entire brain stem. However, we detected reduced connectivity of MTG with several task-positive regions (cingulate, insula, IPL) and increased connectivity between the MTG's task-positive and task-negative subregions. Since multiple atlases parcellate MTG subregions into both task-positive and task-negative networks [52, 55, 78], our findings suggest that the imbalance between these networks may be centered around MTG abnormalities that should be explored further in future research with larger samples of unmedicated patients.

We did not detect rs-FC abnormalities in CSTC circuitry, and specifically had no subcortical findings. This could be due, in part, to methodology. First, while multiband sequences offer excellent cortical spatio-temporal resolution, they have lower signal-to-noise ratios for subcortical (compared to cortical) structures [79]. Second, we included only unmedicated patients, whereas most rs-FC findings of CSTC alterations come from studies that included medicated patients, many receiving serotonin reuptake inhibitors (SRIs). Although the direct effects of SRIs on BOLD signal in individuals with OCD are incompletely understood, SRIs influence BOLD signal in healthy volunteers [80, 81], and patients with OCD exhibit differing rs-FC patterns based on medication status [37]. Furthermore, a large multi-site study of OCD showed that psychotropic medication use exerted significant effects on all measures of brain structure evaluated, and that medication status often had a greater effect size than clinical diagnosis [82]. Thus, medication usage confounds reports of altered connectivity from previous studies of OCD. While some of these studies attempted to identify effect of medication or SRI-refractory disease on findings by including medication status as a covariate or performed post hoc analyses of unmedicated subsamples, these subsamples were small (fewer than 30 patients [12, 36, 39, 71]). Our findings from a larger sample of unmedicated patients, in which rs-FC abnormalities were detected in VAN, salience/CO, and DMN networks but not CSTC circuitry, underscore the importance of separating effects due to medication and those due to the underlying disorder.

Prediction of EX/RP treatment response

Reduced connectivity in the rs-FC component connecting the MTG to task-positive networks (i.e., VAN, salience/CO) predicted greater response to EX/RP in OCD patients. This component was identified and defined based on group (OCD vs. HC) differences. That it also predicted treatment response in patients provides converging evidence that this identified component may play an important role in OCD pathophysiology. However, our prediction findings should be interpreted with caution since they did not replicate when we used an alternate parcellation. We suspect that some of the edges that emerged from our a priori analyses using the Gordon parcellation were between two nodes that are anatomically close together (e.g., R_VentralAttn_13 and R_Default_27, both subregions of the MTG) and likely grouped into the same ROI in the much coarser Schaefer parcellation. Further, we did not have an independent validation sample of participants that would have allowed us to test out-of-sample prediction. Thus, these treatment prediction findings should be interpreted with caution.

Prior work using rsfMRI to predict treatment response has generated mixed results [35, 36], but it is difficult to compare these findings to ours since they did not use whole-brain approaches. Only one prior study employed a whole-brain

approach in 17 unmedicated adults with OCD, reporting that overall connectivity of a subregion of the right basolateral amygdala with the rest of the brain predicted response to EX/RP [38]. The NBS approach used in our study cannot detect findings that affect only portions of a region. Furthermore, the method used in the prior study was designed to detect regions with diffusely altered connectivity with the rest of the brain, rather than strongly altered connectivity with specific regions. In contrast, the NBS approach we employed is sensitive to multiple, overlapping edges that significantly differ between groups.

Strengths

Our study had several strengths. First, we used multiband acquisition sequences and state-of-the-art image processing pipelines (e.g., the HCP pipeline [46]). Second, to address concerns of the impact of head motion on rs-FC data, we conducted motion denoising via nuisance regression with squared terms, temporal derivatives, and squared temporal derivatives for each of six realignment parameters (translation and rotation in each of the *x*, *y*, and *z* planes) based on a recent benchmarking study showing that this 24-parameter method outperformed alternatives with fewer motion-related regressors [48]. We additionally performed motion censoring [49] using relatively strict cutoffs based on FD and DVARS and included FD as a covariate in analyses to further reduce the residual effects of head motion on results. Third, we reproduced our analyses of group differences using two contrasting parcellations, one finer [52] and one coarser [55], suggesting that our results are robust and not an artifact of parcellation scheme. Finally, we enrolled only unmedicated patients with minimal comorbidities, and 34 out of 41 patients (83%) were drug-naïve, minimizing the confound of medication use on our brain findings.

Limitations

Our sample, although comparable to or larger than previous rs-FC studies of unmedicated adults with OCD, was still relatively small and 73% non-Hispanic white. In addition, our study design compared OCD patients undergoing EX/RP therapy with HC participants, but did not have a positive control arm (e.g., an OCD group undergoing placebo or an alternative treatment). Future work should explore neural predictors of treatment response in a large, randomized control trial with EX/RP, medication, and placebo arms to examine specificity. Finally, our study was not powered to test treatment response prediction in an independent validation sample [83], but does set the stage for future studies to examine whether baseline rs-FC centered around the MTG/STG predicts EX/RP response in an independent sample.

Future directions

Comparing findings across neuroimaging studies are difficult due, in part, to differences in methods. To address this challenge, we recommend future rs-FC studies in OCD standardize preprocessing to help with transparency and replication [84] and use whole-brain approaches to expand our understanding of OCD beyond existing models. In addition, we recommend that researchers report ROIs and findings by coordinates rather than just by name or description, make imaging (e.g., NIFTI or CIFTI format) files containing masks of these regions freely available online, and highlight in manuscripts when a network being studied has multiple names. Sensitivity analyses can be used to test if findings replicate across different atlases, as choice of parcellation can influence functional connectivity-based results [53, 54]. Finally, future studies that assess the comparability of multiband rs-FC measurements to those from traditional singleband sequences would be helpful in understanding how newer imaging results compare to prior findings.

CONCLUSIONS

Our study is the first to combine multiband rs-FC with a whole-brain network-based approach to assess rs-FC abnormalities in unmedicated adults with OCD and rs-FC predictors of response to EX/RP. Functional connectivity in a component dominated by edges connecting task-positive temporal gyri regions to other task-positive (salience/CO) and task-negative (DMN) regions was altered in patients with OCD. Furthermore, those patients with lower functional connectivity across these regions showed better response to EX/RP. These findings suggest that altered connectivity across task-positive and task-negative temporal gyri regions may be central to OCD pathophysiology. Since rs-FC is relatively easy to acquire consistently across sites and scanners, this work highlights the need for future rs-FC studies of EX/RP response in unmedicated OCD patients to validate the predictive value of these findings in an independent sample.

FUNDING AND DISCLOSURE

This work was supported by grants from the National Institute of Mental Health (R01MH104648; Principal Investigators: RM and HBS) and the National Institutes of Health (MSTP Training Grant to Columbia University T32GM007367, supporting TCS). In the last 3 years, HBS has received research funds from Biohaven (2018 to present), royalties from Cambridge University Press and UpToDate, Inc., and a stipend for serving as associate editor of JAMA Psychiatry (2019 to present). The remaining authors declare no competing interests.

ACKNOWLEDGEMENTS

We acknowledge and thank Martine Fontaine and all members of the Center for OCD and Related Disorders (e.g., therapists, clinical raters, research assistants, data managers) who worked on this study as well as all research participants. This study has been registered as a clinical trial (Control and Reward Circuits in Obsessive Compulsive Disorder, NCT02221518); additional information is provided at https://clinicaltrials.gov/ct2/show/NCT02221518.

AUTHOR CONTRIBUTIONS

RM and HBS designed the study; TCS, DP, and RM analyzed the data; and all authors contributed to writing and/or editing the manuscript.

ADDITIONAL INFORMATION

Supplementary Information accompanies this paper at (https://doi.org/10.1038/s41386-020-00929-9).

Publisher's note Springer Nature remains neutral with regard to jurisdictional claims in published maps and institutional affiliations.

REFERENCES

1. Maia TV, Cooney RE, Peterson BS. The neural bases of obsessive-compulsive disorder in children and adults. Dev Psychopathol. 2008;20:1251–83.
2. Ahmari SE, Risbrough VB, Geyer MA, Simpson HB. Impaired sensorimotor gating in unmedicated adults with obsessive-compulsive disorder. Neuropsychopharmacology. 2012;37:1216–23.
3. Marsh R, Maia TV, Peterson BS. Functional disturbances within frontostriatal circuits across multiple childhood psychopathologies. Am J Psychiatry. 2009;166:664–74.
4. Graybiel AM, Rauch SL. Toward a neurobiology of obsessive-compulsive disorder. Neuron 2000;28:343–7.
5. Stein DJ, Costa DLC, Lochner C, Miguel EC, Reddy YCJ, Shavitt RG, et al. Obsessive-compulsive disorder. Nat Rev Dis Prim. 2019;5:52.
6. Gursel DA, Avram M, Sorg C, Brandl F, Koch K. Frontoparietal areas link impairments of large-scale intrinsic brain networks with aberrant fronto-striatal interactions in OCD: a meta-analysis of resting-state functional connectivity. Neurosci Biobehav Rev. 2018;87:151–60.

7. Marsh R, Horga G, Parashar N, Wang Z, Peterson BS, Simpson HB. Altered activation in fronto-striatal circuits during sequential processing of conflict in unmedicated adults with obsessive-compulsive disorder. Biol Psychiatry. 2014;75:615–22.
8. Harrison BJ, Soriano-Mas C, Pujol J, Ortiz H, Lopez-Sola M, Hernandez-Ribas R, et al. Altered corticostriatal functional connectivity in obsessive-compulsive disorder. Arch Gen Psychiatry. 2009;66:1189–200.
9. Posner J, Marsh R, Maia TV, Peterson BS, Gruber A, Simpson HB. Reduced functional connectivity within the limbic cortico-striato-thalamo-cortical loop in unmedicated adults with obsessive-compulsive disorder. Hum Brain Mapp. 2014;35:2852–60.
10. Sakai Y, Narumoto J, Nishida S, Nakamae T, Yamada K, Nishimura T, et al. Corticostriatal functional connectivity in non-medicated patients with obsessive-compulsive disorder. Eur Psychiatry. 2011;26:463–9.
11. Zhao Q, Xu T, Wang Y, Chen D, Liu Q, Yang Z, et al. Limbic cortico-striato-thalamo-cortical functional connectivity in drug-naive patients of obsessive-compulsive disorder. Psychol Med. 2019:1–13.
12. Moody TD, Morfini F, Cheng G, Sheen C, Tadayonnejad R, Reggente N, et al. Mechanisms of cognitive-behavioral therapy for obsessive-compulsive disorder involve robust and extensive increases in brain network connectivity. Transl Psychiatry. 2017;7:e1230.
13. Milad MR, Rauch SL. Obsessive-compulsive disorder: beyond segregated cortico-striatal pathways. Trends Cogn Sci. 2012;16:43–51.
14. Cocchi L, Harrison BJ, Pujol J, Harding IH, Fornito A, Pantelis C, et al. Functional alterations of large-scale brain networks related to cognitive control in obsessive-compulsive disorder. Hum Brain Mapp. 2012;33:1089–106.
15. Norman LJ, Carlisi C, Lukito S, Hart H, Mataix-Cols D, Radua J, et al. Structural and functional brain abnormalities in attention-deficit/hyperactivity disorder and obsessive-compulsive disorder: a comparative meta-analysis. JAMA Psychiatry. 2016;73:815–25.
16. Norman LJ, Taylor SF, Liu Y, Radua J, Chye Y, De Wit SJ, et al. Error processing and inhibitory control in obsessive-compulsive disorder: a meta-analysis using statistical parametric maps. Biol Psychiatry. 2019;85:713–25.
17. Gottlich M, Kramer UM, Kordon A, Hohagen F, Zurowski B. Decreased limbic and increased fronto-parietal connectivity in unmedicated patients with obsessive-compulsive disorder. Hum Brain Mapp. 2014;35:5617–32.
18. Cyr M, Pagliaccio D, Yanes-Lukin P, Fontaine M, Rynn MA, Marsh R. Altered network connectivity predicts response to cognitive-behavioral therapy in pediatric obsessive-compulsive disorder. Neuropsychopharmacology. 2020,45:1232–40.
19. Kerns JG, Cohen JD, MacDonald AW 3rd, Cho RY, Stenger VA, Carter CS. Anterior cingulate conflict monitoring and adjustments in control. Science. 2004;303:1023–6.
20. Menon V, Adleman NE, White CD, Glover GH, Reiss AL. Error-related brain activation during a Go/NoGo response inhibition task. Hum Brain Mapp. 2001;12:131–43.
21. Ridderinkhof KR, Ullsperger M, Crone EA, Nieuwenhuis S. The role of the medial frontal cortex in cognitive control. Science. 2004;306:443–7.
22. Dosenbach NU, Fair DA, Miezin FM, Cohen AL, Wenger KK, Dosenbach RA, et al. Distinct brain networks for adaptive and stable task control in humans. Proc Natl Acad Sci U S A. 2007;104:11073–8.
23. Beckmann CF, DeLuca M, Devlin JT, Smith SM. Investigations into resting-state connectivity using independent component analysis. Philos Trans R Soc Lond B Biol Sci. 2005;360:1001–13.
24. Biswal BB, Van Kylen J, Hyde JS. Simultaneous assessment of flow and BOLD signals in resting-state functional connectivity maps. NMR Biomed. 1997;10:165–70.
25. Fox MD, Snyder AZ, Vincent JL, Corbetta M, Van Essen DC, Raichle ME. The human brain is intrinsically organized into dynamic, anticorrelated functional networks. Proc Natl Acad Sci USA. 2005;102:9673–8.
26. Greicius MD, Krasnow B, Reiss AL, Menon V. Functional connectivity in the resting brain: a network analysis of the default mode hypothesis. Proc Natl Acad Sci USA. 2003;100:253–8.
27. Raichle ME, MacLeod AM, Snyder AZ, Powers WJ, Gusnard DA, Shulman GL. A default mode of brain function. Proc Natl Acad Sci USA. 2001;98:676–82.
28. Harrison BJ, Pujol J, Lopez-Sola M, Hernandez-Ribas R, Deus J, Ortiz H, et al. Consistency and functional specialization in the default mode brain network. Proc Natl Acad Sci U S A. 2008;105:9781–6.
29. Mason MF, Norton MI, Van Horn JD, Wegner DM, Grafton ST, Macrae CN. Wandering minds: the default network and stimulus-independent thought. Science 2007;315:393–5.
30. Fan J, Zhong M, Gan J, Liu W, Niu C, Liao H, et al. Altered connectivity within and between the default mode, central executive, and salience networks in obsessive-compulsive disorder. J Affect Disord. 2017;223:106–14.
31. Posner J, Song I, Lee S, Rodriguez CI, Moore H, Marsh R, et al. Increased functional connectivity between the default mode and salience networks in unmedicated adults with obsessive-compulsive disorder. Hum Brain Mapp. 2017;38:678–87.
32. Foa EB, Liebowitz MR, Kozak MJ, Davies S, Campeas R, Franklin ME, et al. Randomized, placebo-controlled trial of exposure and ritual prevention, clomipramine, and their combination in the treatment of obsessive-compulsive disorder. Am J Psychiatry. 2005;162:151–61.
33. Simpson HB, Huppert JD, Petkova E, Foa EB, Liebowitz MR. Response versus remission in obsessive-compulsive disorder. J Clin Psychiatry. 2006;67:269–76.
34. O'Neill J, Feusner JD. Cognitive-behavioral therapy for obsessive-compulsive disorder: access to treatment, prediction of long-term outcome with neuroimaging. Psychol Res Behav Manag. 2015;8:211–23.
35. Fullana MA, Zhu X, Alonso P, Cardoner N, Real E, Lopez-Sola C, et al. Basolateral amygdala-ventromedial prefrontal cortex connectivity predicts cognitive behavioural therapy outcome in adults with obsessive-compulsive disorder. J Psychiatry Neurosci. 2017;42:378–85.
36. Reggente N, Moody TD, Morfini F, Sheen C, Rissman J, O'Neill J, et al. Multivariate resting-state functional connectivity predicts response to cognitive behavioral therapy in obsessive-compulsive disorder. Proc Natl Acad Sci USA. 2018;115:2222–27.
37. Beucke JC, Sepulcre J, Talukdar T, Linnman C, Zschenderlein K, Endrass T, et al. Abnormally high degree connectivity of the orbitofrontal cortex in obsessive-compulsive disorder. JAMA Psychiatry. 2013;70:619–29.
38. Gottlich M, Kramer UM, Kordon A, Hohagen F, Zurowski B. Resting-state connectivity of the amygdala predicts response to cognitive behavioral therapy in obsessive compulsive disorder. Biol Psychol. 2015;111:100–9.
39. Feusner JD, Moody T, Lai TM, Sheen C, Khalsa S, Brown J, et al. Brain connectivity and prediction of relapse after cognitive-behavioral therapy in obsessive-compulsive disorder. Front Psychiatry. 2015;6:74.
40. Pagliaccio D, Middleton R, Hezel D, Steinman S, Snorrason I, Gershkovich M, et al. Task-based fMRI predicts response and remission to exposure therapy in obsessive-compulsive disorder. Proc Natl Acad Sci USA. 2019;116:20346–53.
41. American Psychiatric Association. Diagnostic and statistical manual of mental disorders (DSM-5®). American Psychiatric Pub: Philadelphia; 2013.
42. First MB, Spitzer RL, Gibbon M, Williams JB. SCID-I/P. Biometrics Research, New York State Psychiatric Institute: New York; 2002.
43. Foa EB, Yadin E, Lichner TK. Exposure and response (ritual) prevention for obsessive compulsive disorder: therapist guide. Oxford University Press: New York; 2012.
44. Goodman WK, Price LH, Rasmussen SA, Mazure C, Fleischmann RL, Hill CL, et al. The Yale-Brown Obsessive Compulsive Scale. I. Development, use, and reliability. Arch Gen Psychiatry. 1989;46:1006–11.
45. Van Essen DC, Ugurbil K, Auerbach E, Barch D, Behrens TE, Bucholz R, et al. The Human Connectome Project: a data acquisition perspective. Neuroimage 2012;62:2222–31.
46. Glasser MF, Sotiropoulos SN, Wilson JA, Coalson TS, Fischl B, Andersson JL, et al. The minimal preprocessing pipelines for the Human Connectome Project. Neuroimage 2013;80:105–24.
47. Fair DA, Miranda-Dominguez O, Snyder AZ, Perrone A, Earl EA, Van AN, et al. Correction of respiratory artifacts in MRI head motion estimates. Neuroimage 2020;208:116400.
48. Ciric R, Wolf DH, Power JD, Roalf DR, Baum GL, Ruparel K, et al. Benchmarking of participant-level confound regression strategies for the control of motion artifact in studies of functional connectivity. Neuroimage 2017;154:174–87.
49. Power JD, Barnes KA, Snyder AZ, Schlaggar BL, Petersen SE. Spurious but systematic correlations in functional connectivity MRI networks arise from subject motion. Neuroimage 2012;59:2142–54.
50. Power JD, Schlaggar BL, Petersen SE. Recent progress and outstanding issues in motion correction in resting state fMRI. Neuroimage 2015;105:536–51.
51. Marcus DS, Harwell J, Olsen T, Hodge M, Glasser MF, Prior F, et al. Informatics and data mining tools and strategies for the human connectome project. Front Neuroinform. 2011;5:4.
52. Gordon EM, Laumann TO, Adeyemo B, Huckins JF, Kelley WM, Petersen SE. Generation and evaluation of a cortical area parcellation from resting-state correlations. Cereb Cortex. 2016;26:288–303.
53. Messe A. Parcellation influence on the connectivity-based structure-function relationship in the human brain. Hum Brain Mapp. 2020;41:1167–80.
54. Zalesky A, Fornito A, Harding IH, Cocchi L, Yucel M, Pantelis C, et al. Whole-brain anatomical networks: does the choice of nodes matter? Neuroimage 2010;50:970–83.
55. Schaefer A, Kong R, Gordon EM, Laumann TO, Zuo XN, Holmes AJ, et al. Local-global parcellation of the human cerebral cortex from intrinsic functional connectivity MRI. Cereb Cortex. 2018;28:3095–114.
56. Zalesky A, Fornito A, Bullmore ET. Network-based statistic: identifying differences in brain networks. Neuroimage 2010;53:1197–207.
57. Xia M, Wang J, He Y. BrainNet Viewer: a network visualization tool for human brain connectomics. PLoS ONE. 2013;8:e68910.

58. Le QV, Karpenko A, Ngiam J, Ng AY. ICA with reconstruction cost for efficient overcomplete feature learning. Proceedings of the 24th International Conference on Neural Information Processing Systems. 2011:1017–25.
59. Bates D, Maechler M, Bolker B, Walker S, Christensen RHB, Singmann H, et al. Package 'lme4'. Convergence. 2015;12:2.
60. Beucke JC, Sepulcre J, Eldaief MC, Sebold M, Kathmann N, Kaufmann C. Default mode network subsystem alterations in obsessive-compulsive disorder. Br J Psychiatry. 2014;205:376–82.
61. Chen Y, Meng X, Hu Q, Cui H, Ding Y, Kang L, et al. Altered resting-state functional organization within the central executive network in obsessive-compulsive disorder. Psychiatry Clin Neurosci. 2016;70:448–56.
62. Anticevic A, Hu S, Zhang S, Savic A, Billingslea E, Wasylink S, et al. Global resting-state functional magnetic resonance imaging analysis identifies frontal cortex, striatal, and cerebellar dysconnectivity in obsessive-compulsive disorder. Biol Psychiatry. 2014;75:595–605.
63. Vincent JL, Kahn I, Snyder AZ, Raichle ME, Buckner RL. Evidence for a frontoparietal control system revealed by intrinsic functional connectivity. J Neurophysiol. 2008;100:3328–42.
64. Yeo BT, Krienen FM, Sepulcre J, Sabuncu MR, Lashkari D, Hollinshead M, et al. The organization of the human cerebral cortex estimated by intrinsic functional connectivity. J Neurophysiol. 2011;106:1125–65.
65. Seeley WW, Menon V, Schatzberg AF, Keller J, Glover GH, Kenna H, et al. Dissociable intrinsic connectivity networks for salience processing and executive control. J Neurosci. 2007;27:2349–56.
66. Stern ER, Fitzgerald KD, Welsh RC, Abelson JL, Taylor SF. Resting-state functional connectivity between fronto-parietal and default mode networks in obsessive-compulsive disorder. PLoS ONE. 2012;7:e36356.
67. Power JD, Cohen AL, Nelson SM, Wig GS, Barnes KA, Church JA, et al. Functional network organization of the human brain. Neuron. 2011;72:665–78.
68. Zhang T, Wang J, Yang Y, Wu Q, Li B, Chen L, et al. Abnormal small-world architecture of top-down control networks in obsessive-compulsive disorder. J Psychiatry Neurosci. 2011;36:23–31.
69. Hou JM, Zhao M, Zhang W, Song LH, Wu WJ, Wang J, et al. Resting-state functional connectivity abnormalities in patients with obsessive-compulsive disorder and their healthy first-degree relatives. J Psychiatry Neurosci. 2014;39:304–11.
70. Jang JH, Kim JH, Jung WH, Choi JS, Jung MH, Lee JM, et al. Functional connectivity in fronto-subcortical circuitry during the resting state in obsessive-compulsive disorder. Neurosci Lett. 2010;474:158–62.
71. Sha Z, Edmiston EK, Versace A, Fournier JC, Graur S, Greenberg T, et al. Functional disruption of cerebello-thalamo-cortical networks in obsessive-compulsive disorder. Biol Psychiatry Cogn Neurosci Neuroimaging. 2020;5:438–47.
72. Dosenbach NU, Nardos B, Cohen AL, Fair DA, Power JD, Church JA, et al. Prediction of individual brain maturity using fMRI. Science 2010;329:1358–61.
73. Shin NY, Lee TY, Kim E, Kwon JS. Cognitive functioning in obsessive-compulsive disorder: a meta-analysis. Psychol Med. 2014;44:1121–30.
74. Kalanthroff E, Henik A, Simpson HB, Todder D, Anholt GE. To do or not to do? Task control deficit in obsessive-compulsive disorder. Behav Ther. 2017;48:603–13.
75. Jung J, Cloutman LL, Binney RJ, Lambon, Ralph MA. The structural connectivity of higher order association cortices reflects human functional brain networks. Cortex 2017;97:221–39.
76. Fan J, Zhong M, Gan J, Liu W, Niu C, Liao H, et al. Spontaneous neural activity in the right superior temporal gyrus and left middle temporal gyrus is associated with insight level in obsessive-compulsive disorder. J Affect Disord. 2017;207:203–11.
77. Kim M, Kwak S, Yoon YB, Kwak YB, Kim T, Cho KIK, et al. Functional connectivity of the raphe nucleus as a predictor of the response to selective serotonin reuptake inhibitors in obsessive-compulsive disorder. Neuropsychopharmacology 2019;44:2073–81.
78. Glasser MF, Coalson TS, Robinson EC, Hacker CD, Harwell J, Yacoub E, et al. A multi-modal parcellation of human cerebral cortex. Nature 2016;536:171–78.
79. Barch DM, Burgess GC, Harms MP, Petersen SE, Schlaggar BL, Corbetta M, et al. Function in the human connectome: task-fMRI and individual differences in behavior. Neuroimage 2013;80:169–89.
80. McCabe C, Mishor Z, Filippini N, Cowen PJ, Taylor MJ, Harmer CJ. SSRI administration reduces resting state functional connectivity in dorso-medial prefrontal cortex. Mol Psychiatry. 2011;16:592–4.
81. Simmons AN, Arce E, Lovero KL, Stein MB, Paulus MP. Subchronic SSRI administration reduces insula response during affective anticipation in healthy volunteers. Int J Neuropsychopharmacol. 2009;12:1009–20.
82. van den Heuvel OA, Boedhoe PSW, Bertolin S, Bruin WB, Francks C, Ivanov I, et al. An overview of the first 5 years of the ENIGMA obsessive-compulsive disorder working group: the power of worldwide collaboration. Hum Brain Mapp. 2020.
83. Poldrack RA, Huckins G, Varoquaux G. Establishment of best practices for evidence for prediction: a review. JAMA Psychiatry. 2020;77:534–40.
84. Simmons JP, Nelson LD, Simonsohn U. False-positive psychology: undisclosed flexibility in data collection and analysis allows presenting anything as significant. Psychol Sci. 2011;22:1359–66.
85. Lancaster JL, Rainey LH, Summerlin JL, Freitas CS, Fox PT, Evans AC, et al. Automated labeling of the human brain: a preliminary report on the development and evaluation of a forward-transform method. Hum Brain Mapp. 1997;5:238–42.
86. Lancaster JL, Woldorff MG, Parsons LM, Liotti M, Freitas CS, Rainey L, et al. Automated Talairach atlas labels for functional brain mapping. Hum Brain Mapp. 2000;10:120–31.